

# Control of entanglement and two-qubit quantum gates with atoms passing through a detuned optical cavity

D. Gonta<sup>1,\*</sup> and S. Fritzsche<sup>2,3,†</sup>

<sup>1</sup>*Max-Planck-Institut für Kernphysik, Postfach 103980, D-69029 Heidelberg, Germany*

<sup>2</sup>*Physikalisches Institut der Universität Heidelberg, D-69120 Heidelberg, Germany*

<sup>3</sup>*Gesellschaft für Schwerionenforschung (GSI), D-64291 Darmstadt, Germany*

(Dated: May 29, 2019)

A scheme is proposed to generate an entangled state between two effectively interacting ( $\Lambda$ -type) four-level atoms, for which the effective interaction is produced by an off-resonant optical cavity and a laser beam that acts perpendicular to the cavity axis. It is shown how the degree of entanglement depends on the atomic velocity and the (initial) distance between the atoms. In addition, schemes are suggested to implement various two-qubit gates within the framework of proposed atom-cavity-laser setups, such as the *i*-swap gate, controlled-*Z* gate, and the controlled- $\overline{\text{NOT}}$  gate. For all these schemes, we display the atomic velocities and inter-atomic distances for which these gates are realized.

PACS numbers: 42.50.Pq, 42.50.Dv, 03.67.Mn

## I. INTRODUCTION

During recent years, quantum entanglement has been found important not only in studying the non-classical behavior of composite systems but also as one essential resource for the engineering and processing of quantum information. Nowadays, there are indeed various applications known that (would) greatly benefit from having entangled quantum states available as, for instance, superdense coding [1], quantum cryptography [2], or the use of Grover's quantum search algorithm [3], to name just a few of them. Despite of the recent progress in dealing with composite quantum systems, however, their manipulation and controlled interaction with the environment has remained a challenge for experiment until the present. Apart from various other implementations of composite systems, the proof for an excellent control about the generation of entanglement has been achieved especially with neutral atoms that are coupled to a high-finesse optical cavity [4, 5, 6].

From the experimental perspective, there are two basic types of (atomic) level configurations utilized to encode and store a single qubit: Apart from (i) the use of *optical* qubits, that simply refer to (two) atomic levels separated by an optical transition frequency, one may (ii) utilize also the (so-called) *hyperfine* qubits that are associated with two hyperfine levels of—usually—the electronic ground state of the atoms. In neutral atoms, these hyperfine levels are typically separated by a microwave frequency and are known to be robust with regard to decoherence effects and external stray fields in contrast to the optical qubits mentioned above. For the hyperfine qubits, therefore, rather long coherence times ( $\sim 1$  s) have been reported in the literature [7, 8] even while

transporting the atoms over macroscopic distances [9]. In addition, a number of microwave techniques have been developed during the last decades in order to define, manipulate and detect the state of such hyperfine qubits [7, 8, 9, 10, 11, 12].

Unfortunately, however, a (atomic) hyperfine qubit cannot couple directly to a cavity with mode frequencies in the optical domain. Therefore, in order to manipulate the information encoded by the atom, the superposition of the hyperfine levels must first be transferred coherently to some other (electronically) excited states, before the atom enters the cavity, and this information must be brought back also in a controlled fashion after the atom has exited the cavity. Instead of an atomic two-level configuration, we then need to consider a four-level scheme, in which the two hyperfine levels for storing the quantum information are associated with two (additional) optically excited levels. Moreover, in order to realize an efficient atom-cavity coupling, the energy splitting of the two electronically excited levels should be compatible with the frequency of the cavity mode(s). In this way, a coupling between the hyperfine qubit and the optical cavity mode can be achieved indeed and may open a route towards the implementation of quantum gates via cavity-mediated atom-atom interactions.

A significant progress in understanding the formation of entanglement between two four-level atoms coupled to an optical cavity and an external laser beam, has been made recently by You and co-authors [13] who utilized a novel cavity-mediated atom-atom interaction regime [14]. This regime is based on the stimulated exchange of a photon between two bi-level atoms and the cavity mode that is tuned off-resonantly with regard to the atomic transition frequency. In Ref. [15], it was later shown experimentally that this effective atom-atom interaction can lead to the generation of entanglement between two atoms that cross a detuned cavity. The theoretical predictions made by You *et al.* with regard to entanglement formation, however, rely on the assumption that both atoms couple to the cavity mode by a constant coupling strength while

---

\*Electronic address: gonta@physi.uni-heidelberg.de

†Electronic address: s.fritzsche@gsi.de

crossing it. In reality, the atoms cross the cavity being separated by a macroscopic distance, which implies that atoms have different atom-cavity couplings as given by the radiation pattern of the cavity standing-wave. Therefore, a more detailed description of the cavity-mediated atomic entanglement generation has to be considered, in which the entanglement between the atoms depend also on the atom-cavity coupling which depends, in turn, on the location of both atoms inside the cavity mode. Such a position-dependent coupling between the atom and the cavity requires an extension of the previous theoretical predictions and suggests that the degree of entanglement, that is finally obtained, might depend substantially on the details of how the atoms cross the cavity in the course of interaction.

In the present work, we propose a more realistic scheme to generate an entangled state between the hyperfine qubits of two four-level atoms with a  $\Lambda$ -type level configuration. In this scheme, the effective interaction between the atoms is mediated by an optical cavity and a laser beam that acts perpendicular to the cavity axis. Moreover, we assume the atoms to be separated from each other by a macroscopic distance, and *no direct* interaction between the atoms occurs. However, both atoms are simultaneously affected by the laser field and interact with the same cavity mode while passing through the cavity. This scheme gives rise to an cavity-laser mediated *effective* atom-atom interaction for the cavity acting off-resonantly with respect to the atomic transition frequency (optical levels). The two parameters to control the interaction are the velocity and inter-atomic distance between the atoms. For two atoms being initially prepared in a product state (of their hyperfine qubits), we determine those velocities and distances for which the atoms become maximally entangled when passing through the proposed set-up. Apart from generating entanglement between the atoms, we also suggest schemes to implement various two-qubit quantum logical gates, such as the i-swap gate, controlled-Z gate, and controlled- $\overline{\text{NOT}}$  gate. All these gates can be implemented within the given framework, and the respective velocity and inter-atomic distance of the atoms are discussed, for which the gate fidelities become maximal.

The paper is organized as follows. In the next section, we introduce the scheme to entangle the hyperfine qubits of two four-level atoms. This includes the theoretical description of the effective atom-atom interaction evolution that allows to control this interaction in practice. In Sec. II A, in particular, we present and explain all the steps necessary within the proposed (experimental) set-up, while a more detailed view on this effective interaction is given in Sec. II B by using the adiabatic elimination procedure. In Sec. III, then, the schemes for the implementation of the i-swap, controlled-Z, and controlled- $\overline{\text{NOT}}$  gates are presented and discussed. A few conclusions are finally given in Sec. IV.

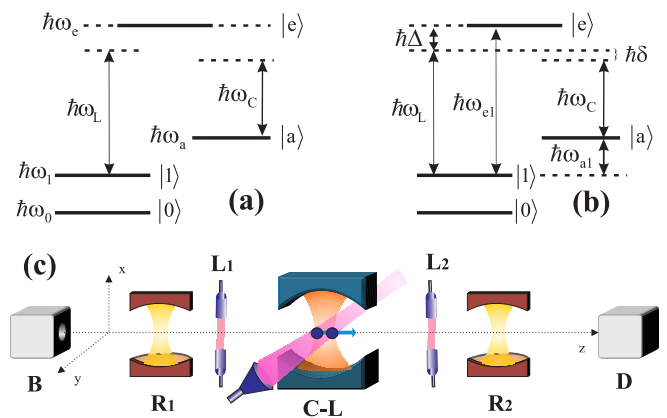


FIG. 1: (Color online) The atomic four-level  $\Lambda$ -type configuration in (a) the Schrödinger picture and (b) the interaction picture. (c) Schematic setup of the experiment. Two neutral atoms from a source  $B$  are supposed to pass through a Ramsey zone  $R_1$ , a pair of Raman laser beams  $L_1$ , an optical cavity  $C$  with a perpendicularly laser beam  $L$  as well as through a second pair of Raman lasers  $L_2$  and Ramsey zone  $R_2$ , before the hyperfine states of the atoms is detected at the detector  $D$ .

## II. GENERATION OF TWO-ATOM ENTANGLEMENT BY AN OPTICAL CAVITY

In this section, we propose and explain our scheme to entangle the hyperfine qubits of two four-level atoms if they were initially prepared in a product state. We hereby assume that the atoms can be controlled with regard to their separation and velocity when they enter the experimental setup as displayed in Fig. 1(c).

### A. Off-Resonant Atom-Cavity interaction

Let us start by considering an atom with a  $\Lambda$ -type four-level configuration as displayed in Fig. 1(a). In this level configuration, the two (hyperfine) states  $|0\rangle$  and  $|1\rangle$  of the atomic ground levels carry the qubit information and are supplemented by the two electronically excited states  $|a\rangle$  and  $|e\rangle$  that are separated from each other by an optical transition frequency. Below, we assume to have two identical atoms  $A_1$  and  $A_2$  of such a  $\Lambda$ -type configuration, and that they are initially prepared in the state  $|0, \bar{1}\rangle \equiv |0\rangle \times |\bar{1}\rangle$ . In this notation, the bar in  $|\bar{\alpha}\rangle$  refers to atom  $A_2$ , and the atoms are taken to be separated by a macroscopic distance  $\ell$  which is large enough that they do not interact directly with each other. Both atoms move with the same (constant) velocity  $\vec{v}$  along the  $z$  axis [see Fig. 1(c)]. Before atom  $A_1$  enters the cavity, the electronic population in state  $|0\rangle$  is excited to the state  $|a\rangle$  by using a pair of laser beams which are weakly coupled to the atomic transitions  $|0\rangle \leftrightarrow |e\rangle$  and  $|e\rangle \leftrightarrow |a\rangle$ , respectively. Such a transfer in the population of atomic levels

by means of non-resonantly tuned laser pulses is known as the two-photon Raman transition [16] that enables one to perform a second-order transition between the states  $|0\rangle$  and  $|a\rangle$ . Below, we shall refer to this population transfer briefly as a Raman pulse and will distinguish between the Raman pulses (laser beams)  $L_1$  and  $L_2$  in front and behind the cavity [see Fig. 1(c)]; also in the time-evolution diagram in Fig. 2, these Raman pulses are displayed as boxed pink circles. We conclude that the purpose of these Raman pulses is just to transfer the electronic population from hyperfine state  $|0\rangle$  to the optical level  $|a\rangle$  in the  $L_1$  zone, and back from  $|a\rangle$  to  $|0\rangle$  in  $L_2$ . The same Raman pulses are applied also to the atom  $A_2$  which follows subsequently with distance  $\ell$ . However, since the atom  $A_2$  enters the set-up in the state  $|\bar{1}\rangle$ , it remains unaffected by the Raman pulse  $L_1$  and, thus, the two atoms enter the cavity in the product state  $|a, \bar{1}\rangle$ .

Inside the cavity, both atoms  $A_1$  and  $A_2$  are coupled via the optical transition  $|a\rangle \leftrightarrow |e\rangle$  (or  $|\bar{a}\rangle \leftrightarrow |\bar{e}\rangle$ , respectively) to the same cavity mode with the frequency  $\omega_C$  [see Fig. 1(a)]. As discussed above, a more realistic description of the atom-cavity interaction evolution is based on the position-dependent atom-cavity coupling

$$g(\vec{r}) = g_o \exp(-|\vec{r}|^2/w^2), \quad (1)$$

where  $g_o$  denotes the vacuum Rabi frequency and  $w$  the (so-called) cavity mode waist, that is the minimum width of the radiation pattern given by the cavity standing-wave [see Fig. 1(c)]. For the two atoms which move through the cavity with the velocity  $\vec{v}$  along the  $z$  axis, the Gaussian profile (1) gives rise to the time-dependent atom-cavity coupling  $g_1(t) \equiv g(z_1^o + vt)$  and  $g_2(t) \equiv g(z_2^o + vt)$ , and where  $z_1^o - z_2^o = \ell > 0$  denote the initial distance between the atoms far enough from the cavity.

The purely cavity-mediated atom-atom interaction (i.e., without the laser beam  $L$ ) is based on the exchange of a *single* photon between the atoms prepared in the product state  $|a, \bar{e}\rangle$ ; this photon exchange can be understood as the emission of a virtual photon into the cavity by the atom  $A_2$  and the re-absorption of the photon by the atom  $A_1$ , while both atoms are coupled off-resonantly to the same cavity mode. An off-resonant atom-cavity interaction hereby refers to the case when the difference (or the detuning) between the atomic  $|a\rangle \leftrightarrow |e\rangle$  transition frequency and the frequency of the cavity mode  $\omega_L$  is large enough,  $|\omega_C - (\omega_e - \omega_a)| \gg |g_\mu(t)|$ , so that only a virtual atom-cavity energy exchange can occur [14].

In our present scheme, in contrast, the atoms enter the cavity in the state  $|a, \bar{1}\rangle$ , and a further intermediate process  $|a, \bar{1}\rangle \rightarrow |a, \bar{e}\rangle$  will first be necessary to obtain the state  $|a, \bar{e}\rangle$ . For this reason, the atoms have to be exposed to a laser beam that acts transversally to the cavity axis and *in addition* to their interaction with the cavity mode, cf. Fig. 1(c). The laser frequency  $\omega_L$  is chosen in order to couple the laser to the atomic transitions  $|1\rangle \leftrightarrow |e\rangle$  and  $|\bar{1}\rangle \leftrightarrow |\bar{e}\rangle$ , respectively, as shown in Fig. 1(a). The position-dependent atom-laser coupling  $\Omega(\vec{r}) = \Omega_o \exp(-|\vec{r}|^2/\tilde{w}^2)$  hereby implies a

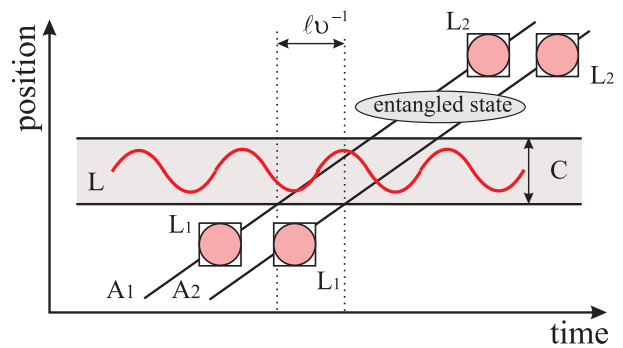


FIG. 2: (Color online) Temporal sequence of steps that need to be carried out in order to generate an entangled state for the two hyperfine qubits of atoms  $A_1$  and  $A_2$ . The grey rectangular area  $C$  denotes the spatial extent of the cavity. The (pink) boxed circles, denoted as  $L_1$  and  $L_2$ , refer to the two (pairs of) Raman laser beams in front and behind the cavity. The two atomic qubits are entangled with each other when both atoms have left the cavity.

further time-dependent coupling for each atom, namely  $\Omega_1(t) \equiv \Omega(z_1^o + vt)$  and  $\Omega_2(t) \equiv \Omega(z_2^o + vt)$ , and where the waist of the atom-laser coupling  $\tilde{w}$  is assumed to be much larger than for the optical cavity. With this coupling of the atoms to both, the laser and the cavity mode, the composite state  $|a, \bar{1}\rangle$  of the two atoms can be manipulated, and it becomes possible to generate an entanglement between the atoms in a similar way as have been suggested by You and coworkers. The latter is based on the sequence of four steps

$$|a, \bar{1}; n\rangle \rightarrow |a, \bar{e}; n\rangle \begin{cases} \nearrow |a, \bar{a}; n+1\rangle \\ \searrow |e, \bar{e}; n-1\rangle \end{cases} \rightarrow |e, \bar{a}; n\rangle \rightarrow |1, \bar{a}; n\rangle,$$

which can be identified for the overall atom-cavity state, if there were  $n$  photons initially in the cavity mode. As seen above, this sequence contains in its middle part a virtual process in which a photon is emitted by one and is absorbed by the second atom, so that the final state of the atoms is independent of number of cavity photons. For an initially empty cavity, we can therefore simplify the sequence to

$$|a, \bar{1}; 0\rangle \rightarrow |a, \bar{e}; 0\rangle \rightarrow |a, \bar{a}; 1\rangle \rightarrow |e, \bar{a}; 0\rangle \rightarrow |1, \bar{a}; 0\rangle. \quad (2)$$

Therefore, if we omit to display the intermediate states in the sequence (2), the laser and cavity field together produces an *effective* atom-atom interaction  $|a, \bar{1}\rangle \xrightarrow{L, C} |1, \bar{a}\rangle$  between the initial and final atomic states, and where the state of the cavity field is factorized out. With this effective interaction, the maximally entangled state

$$|\Phi\rangle = \frac{1}{\sqrt{2}} (|a, \bar{1}\rangle + e^{i\varphi}|1, \bar{a}\rangle) \quad (3)$$

can be generated in a straightforward way by tuning the atomic velocity  $v$  and the inter-atomic distance  $\ell$  for a

given set of cavity-laser parameters:  $\omega_C$ ,  $\omega_L$ ,  $w$ ,  $g_o$ , and  $\Omega_o$ . In the next subsection, we shall analyze in more details how this effective atom-atom interaction depends on the velocity and distance of the atoms, while they are passing through the cavity.

After the atoms  $A_1$  and  $A_2$  have both left the cavity, their superposition of the (electronically) excited states  $|a\rangle$  and  $|\bar{a}\rangle$  must be transferred back to the (ground) hyperfine levels  $|0\rangle$  and  $|\bar{0}\rangle$  in order to protect them from decoherence because of the spontaneous decay of these excited levels. Similar to the initial excitation of the state  $|a\rangle$ , this is achieved by applying a (second) Raman pulse  $L_2$  behind the cavity [see Fig. 1(c)]. The entangled state (3) is then mapped upon the state

$$|\Phi'\rangle = \frac{1}{\sqrt{2}} (|0, \bar{1}\rangle + e^{i\varphi}|1, \bar{0}\rangle). \quad (4)$$

All the steps we have described above in dealing with the two atoms before, while and after they have passed through the cavity are summarized graphically in Fig. 2 by displaying the spatio-temporal evolution of the atoms and the cavity.

### B. Time-Evolution of the Effective Atom-Atom Interaction

While the sequence (2) provides a first idea of how an effective coupling can be achieved between the atoms (and without that they have interacted directly with each other at any time before), we need to analyze these step in further details in order to understand and control this coupling in practice. For this analysis, we shall use the so-called *adiabatic elimination* procedure (see Refs. [14, 17] and Ref. [18] for another derivation) which enables one to exclude all the intermediate degrees of freedom that couple two atoms due to the action of the cavity mode and the laser field.

Formally, the time evolution of the coupled atom-cavity-laser system is driven by the Hamiltonian

$$H = H_1 + H_2 + H_C, \quad (5)$$

where ( $\hbar = 1$ ,  $\mu = 1, 2$ )

$$H_\mu = \omega_1|1\rangle_\mu\langle 1| + \omega_e|e\rangle_\mu\langle e| + \omega_a|a\rangle_\mu\langle a| + \frac{1}{2} [\Omega_\mu(t)e^{-i\omega_L t}|e\rangle_\mu\langle 1| + g_\mu(t)c|e\rangle_\mu\langle a| + h.c.];$$

describes the atom  $A_\mu$  and its interaction with the cavity and laser field, and where

$$H_C = \omega_C c^\dagger c,$$

refers to the cavity mode energy. In the atomic Hamiltonian (5), hereby  $\hbar\omega_1$ ,  $\hbar\omega_e$ , and  $\hbar\omega_a$  are the (excitation) energies of atomic states  $|1\rangle$ ,  $|e\rangle$  and  $|a\rangle$  [see Fig. 1(a)], while  $c$  and  $c^\dagger$  denote the annihilation and creation operators for a photon in the cavity mode, which act upon the Fock states  $|n\rangle$ .

In order to simplify the evaluation of the Schrödinger equation that is associated with the Hamiltonian (5), let us switch here to the interaction picture given by [13]

$$U_{int}^0 = e^{-i(\omega_1 + \omega_L)t} \sum_\mu |e\rangle_\mu \langle e| e^{-i\omega_1 t} \sum_\mu |1\rangle_\mu \langle 1| \times e^{-i\omega_a t} \sum_\mu |a\rangle_\mu \langle a| e^{-i[\omega_L - (\omega_a - \omega_1)]t} c^\dagger c. \quad (6)$$

In this picture, the atom-cavity-laser interaction Hamiltonian becomes

$$H_{int} = -\delta c^\dagger c - \Delta \sum_\mu |e\rangle_\mu \langle e| + \frac{1}{2} \sum_\mu [\Omega_\mu(t)|e\rangle_\mu \langle 1| + g_\mu(t)c|e\rangle_\mu \langle a| + h.c.], \quad (7)$$

where  $\Delta = \omega_L - \omega_{e1}$  and  $\delta = \omega_L - \omega_C - \omega_{a1} = (\omega_L - \omega_{e1}) - (\omega_C - \omega_{ea})$  refer to the off-resonance shifts (detuning) of the laser and cavity frequencies as depicted in Fig. 1(b).

The Hamiltonian (7) drives the state of the composite atom-cavity-laser system due to the Schrödinger equation

$$i \frac{d|\Psi(t)\rangle}{dt} = H_{int}|\Psi(t)\rangle, \quad (8)$$

where the (composite) wave function  $|\Psi(t)\rangle$  is defined in the product space of three (sub)systems:  $A_1(|1\rangle, |e\rangle, |a\rangle)$ ,  $A_2(|\bar{1}\rangle, |\bar{e}\rangle, |\bar{a}\rangle)$ , as well as the cavity Fock states  $C(|0\rangle, |1\rangle)$ . Moreover, by taking into account the composite states that occur in sequence (2), we may restrict this wave function to the subspace

$$|\Psi(t)\rangle = C_1(t)|a, \bar{1}; 0\rangle + C_2(t)|a, \bar{e}; 0\rangle + C_3(t)|a, \bar{a}; 1\rangle + C_4(t)|e, \bar{a}; 0\rangle + C_5(t)|1, \bar{a}; 0\rangle, \quad (9)$$

for which the Schrödinger equation (8) gives rise to the set of equations

$$\begin{aligned} i\dot{C}_1(t) &= \frac{1}{2}\Omega_2(t)C_2(t), \\ i\dot{C}_2(t) &= -\Delta C_2(t) + g_2(t)C_3(t) + \frac{1}{2}\Omega_2(t)C_1(t), \\ i\dot{C}_3(t) &= -\delta C_3(t) + g_1(t)C_4(t) + g_2(t)C_2(t), \\ i\dot{C}_4(t) &= -\Delta C_4(t) + g_1(t)C_3(t) + \frac{1}{2}\Omega_1(t)C_5(t), \\ i\dot{C}_5(t) &= \frac{1}{2}\Omega_1(t)C_4(t), \end{aligned} \quad (10)$$

and where the dot denotes the time derivative.

The off-resonant regime of the atom-cavity and atom-laser interactions, we assumed above, implies

$$|\delta| \gg |g_\mu(t)|, \quad |\Delta| \gg |\Omega_\mu(t)|, \quad |\delta \Delta| \gg |g_\mu^2(t)|. \quad (11)$$

These conditions, therefore, justify the adiabatic elimination procedure for a sufficiently slow-varying time-dependent atom-cavity  $g_\mu(t)$  and atom-laser coupling  $\Omega_\mu(t)$ . By this procedure, the functions  $C_2(t)$ ,  $C_3(t)$ ,

and  $C_4(t)$ , which correspond to the state vectors  $|a, \bar{e}; 0\rangle$ ,  $|a, \bar{a}; 1\rangle$ , and  $|e, \bar{a}; 0\rangle$ , respectively, can be excluded from the set of Eqs. (10). Here, we shall omit the details of the derivation for which the reader is referred to the literature [13, 14, 17, 18]. The remaining two Eqs. for  $C_1(t)$  and  $C_2(t)$  then take the form

$$i\dot{C}_1(t) = \frac{\Omega_2^2(t)}{4\Delta} C_1(t) + \lambda(t) C_5(t), \quad (12a)$$

$$i\dot{C}_5(t) = \lambda(t) C_1(t) + \frac{\Omega_1^2(t)}{4\Delta} C_5(t), \quad (12b)$$

where

$$\lambda(t) = \frac{\Omega_1(t)\Omega_2(t)g_1(t)g_2(t)}{4\delta\Delta^2}$$

is the effective coupling frequency between the initial and final composite states  $|a, \bar{1}; 0\rangle$  and  $|1, \bar{a}; 0\rangle$ , respectively.

The atom-laser coupling  $\Omega_\mu(t)$  is determined by the interaction of the electric-dipole of the atom with the field of the laser. However, since the waist of the laser beam was assumed to be much larger than those of the cavity mode, we may take  $\Omega_\mu(t) = \Omega = \text{const.}$  and include the time-variation only for the atom-cavity coupling  $g_\mu(t)$ . With this assumption in mind, an analytical solution of Eqs. (12) can be obtained in the form

$$|\Psi(t)\rangle = e^{-i\frac{\Omega^2}{4\Delta}t} |\Phi(t)\rangle \quad (13)$$

with

$$|\Phi(t)\rangle = \cos\xi(t)|a, \bar{1}\rangle - i\sin\xi(t)|1, \bar{a}\rangle, \quad (14)$$

if the wave-function  $|\Psi(t)\rangle$  was prepared initially in the product state  $|a, \bar{1}; 0\rangle$ . In the expression (14), moreover, the cavity field has been factorized out in its vacuum state and the effective atom-atom *coupling angle* is defined by

$$\xi(t) = \int_{-\infty}^t \lambda(s) ds.$$

The wave function (14) describes in general an entangled state for the atoms  $A_1$  and  $A_2$ , whose time evolution can be obtained also from the effective (atomic) Hamiltonian

$$H_{\text{eff}} = \lambda(t) (\sigma_1^- \sigma_2^+ + \sigma_1^+ \sigma_2^-), \quad (15)$$

where  $\sigma_\mu^+ = |1\rangle_\mu\langle a|$  and  $\sigma_\mu^- = |a\rangle_\mu\langle 1|$  denote the two-photon atomic excitation and de-excitation operators. Owing to its obvious simplicity, this Hamiltonian provides of course a much better understanding of the effective two-atom evolution (14) that is mediated by the cavity-laser fields and by using the ansatz (9) within the adiabatic regime. Below, we shall restrict ourselves to the evolution of the function  $|\Phi(t)\rangle$  since the Hamiltonian that drives the wave function  $|\Psi(t)\rangle$  differs from (15) by just the constant term  $H_0 = \frac{\Omega^2}{4\Delta} (|1\rangle\langle 1| + |\bar{1}\rangle\langle \bar{1}|)$ . This

factor need not to be considered since we could utilize a modified interaction picture given by the unitary transformation  $U_{int}^1 = \exp(-iH_0t)$ , for which the (original) wave function (13) would coincide with (14).

When both atoms have left the cavity (which is formally obtained in the limit  $t \rightarrow +\infty$ ), the state (14) becomes

$$|\Phi_{+\infty}\rangle = \cos\theta(v, \ell) |a, \bar{1}\rangle - i\sin\theta(v, \ell) |1, \bar{a}\rangle, \quad (16)$$

and where the asymptotic coupling angle is given by

$$\theta(v, \ell) \equiv \xi(+\infty) = \sqrt{\frac{\pi}{32}} \frac{\Omega^2 g_o^2 w}{\delta \Delta^2 v} \exp\left(-\frac{\ell^2}{2w^2}\right).$$

Note that, according to our scheme in Fig. 2, the atomic states  $|a\rangle$  and  $|\bar{a}\rangle$  were mapped in this limit also into the hyperfine states  $|0\rangle$  and  $|\bar{0}\rangle$  by applying a Raman pulse  $L_2$  after the atoms have crossed the cavity. Therefore, the requested limit  $t \rightarrow +\infty$  then implies a mapping of the wave-function (16) into

$$|\Phi'_{+\infty}\rangle = \cos\theta(v, \ell) |0, \bar{1}\rangle - i\sin\theta(v, \ell) |1, \bar{0}\rangle \quad (17)$$

as searched for the atoms  $A_1$  and  $A_2$ .

From Eq. (17), we can easily read off the condition  $\theta(v, \ell) = (2n+1)\pi/4$ , with  $n$  being an integer, for which the two atoms become maximally entangled with each other initially being prepared in the product state  $|a, \bar{1}\rangle$ . For a fixed set of cavity-laser parameters ( $\delta$ ,  $\Delta$ ,  $w$ ,  $g_o$  and  $\Omega$ ), this condition implies that the values of atomic velocity  $v$  and inter-atomic distances  $\ell$  cannot be chosen arbitrarily but must follow the (so-called) *lines of maximal entanglement* displayed in Fig. 3(a) for  $n = 0, 1, 2, 3, 4$ . According to this figure, the change between the (completely) entangled and disentangled state occurs more and more rapidly as the velocity is decreased (or  $n$  increases). For the practical implementation of the scheme above, therefore, the velocities and distances along the (blue)  $n = 0$  line appears to be most appropriate. In Fig. 3(a), all velocities are given in units of  $\Omega^2 g_o^2 w / \delta \Delta^2$  and all distances in units of the cavity waist  $w$ . For typical atom-cavity-laser parameters, say,  $\delta = 20$  MHz,  $\Delta = 1600$  MHz,  $g_o = 27$  MHz,  $\Omega = 50$  MHz, and  $w = 13 \mu\text{m}$ , these velocity and distance units take the values of 0.46 m/s and 13  $\mu\text{m}$ , respectively. These values are compatible with the velocities in the range 0.01,  $\dots$ , 1 m/s which were utilized in recent cavity QED experiments [19, 20, 21], in which atoms are coherently transported in a optical lattice trap (conveyor belt).

Next, let us analyze how sensitive the entanglement depends on the velocity  $v$  and distance  $\ell$  of the atoms. To display the variations in the degree of entanglement, Fig. 3(b) shows the *von Neumann entropy* [22]

$$\begin{aligned} E(v, \ell) &\equiv -\text{Tr}[\rho(v, \ell) \log_2 \rho(v, \ell)] \\ &= -\cos^2\theta(v, \ell) \log_2[\cos^2\theta(v, \ell)] \\ &= -\sin^2\theta(v, \ell) \log_2[\sin^2\theta(v, \ell)], \end{aligned} \quad (18)$$

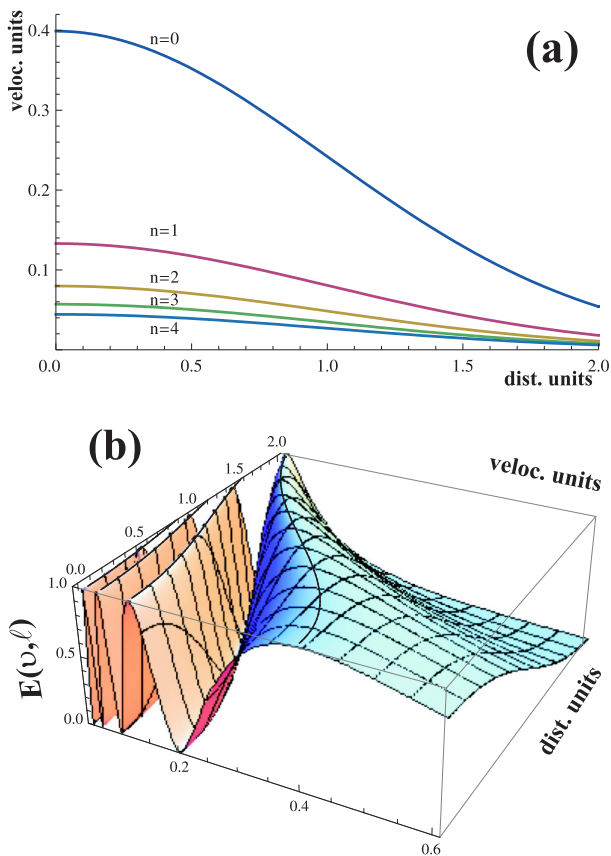


FIG. 3: (Color online) (a) Atomic velocities  $v$  and inter-atomic distances  $\ell$  for which the initial product state  $|a, \bar{1}\rangle$  becomes maximally entangled due to the cavity-laser mediated atom-atom interaction. The velocity  $v$  is displayed in units of  $\Omega^2 g_s^2 w / \delta \Delta^2$  and the inter-atomic distance in units of  $w$ . Along the lines, the condition  $\theta(v, \ell) = (2n + 1)\pi/4$  is satisfied for the asymptotic couplings angle with  $n = 0, 1, 2, 3, 4$ . (b) Von Neumann entropy  $E(v, \ell)$  as function of the atomic velocity  $v$  and inter-atomic distance  $\ell$  (using the same units).

where  $\rho(v, \ell) = \text{Tr}_2(|\Phi'_{+\infty}\rangle\langle\Phi'_{+\infty}|)$  denotes the reduced density operator of the first hyperfine qubit [see Eq. (17)]. The maximal values of the von Neumann entropy, i.e.,  $E(v, \ell) = 1$ , are obtained for the velocities and distances as shown in Fig. 3(a).

Since the atom-atom interaction sequence (2) can be easily reversed (in time) to

$$|1, \bar{a}; 0\rangle \rightarrow |e, \bar{a}; 0\rangle \rightarrow |a, \bar{a}; 1\rangle \rightarrow |a, \bar{e}; 0\rangle \rightarrow |a, \bar{1}; 0\rangle$$

we can generate also the state (for  $t \rightarrow +\infty$ )

$$|\tilde{\Phi}'_{+\infty}\rangle = \cos\theta(v, \ell) |1, \bar{a}\rangle - i \sin\theta(v, \ell) |a, \bar{1}\rangle, \quad (19)$$

from the atoms initially being prepared in the product state  $|1, \bar{a}\rangle$ . Together with the Raman pulse  $L_2$  that maps back the atomic states  $|a\rangle \rightarrow |0\rangle$  and  $|\bar{a}\rangle \rightarrow |\bar{0}\rangle$ , we then obtain the state

$$|\tilde{\Phi}'_{+\infty}\rangle = \cos\theta(v, \ell) |1, \bar{0}\rangle - i \sin\theta(v, \ell) |0, \bar{1}\rangle. \quad (20)$$

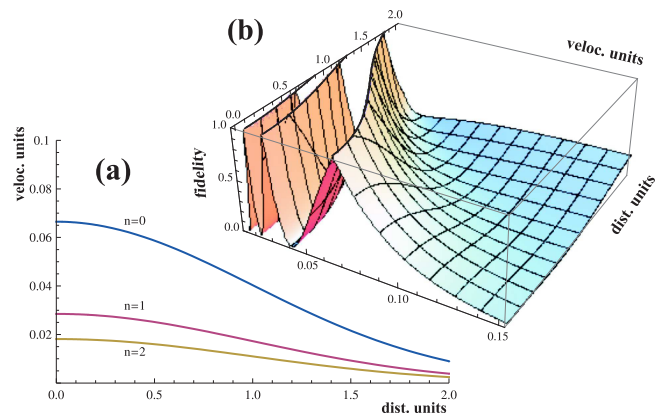


FIG. 4: (Color online) (a) Combinations of the atomic velocity  $v$  and inter-atomic distance  $\ell$  that realizes the i-swap gate (23), i.e., for which the condition (24) is fulfilled for  $n = 0, 1, 2$ . (b) Fidelity  $F_{\text{iswap}}(v, \ell)$  as function of the atomic velocity  $v$  and inter-atomic distance  $\ell$ . The same units of  $v$  and  $\ell$  are used as in Fig. 3.

For the other two initial (product) states  $|a, \bar{a}\rangle$  and  $|1, \bar{1}\rangle$ , in contrast, no effective interaction occurs on the atoms when they pass through the cavity-laser system. From this fact and Eqs. (16), (19), we conclude that the effective Hamiltonian (15) gives a complete description of the (effective) atom-atom interaction for all four possible initial product states of the two atoms being mediated by the cavity-laser fields in the adiabatic regime.

### III. TWO-QUBIT QUANTUM LOGIC GATES

In the previous section, we have shown how the atomic hyperfine qubits of the two atoms  $A_1$  and  $A_2$  can be manipulated adiabatically by means of the atom-cavity-laser setup of Figs. 1(b) and 2. Independent of the initial state of the qubits, the evolution of the two-qubit hyperfine input state  $|\psi_{\text{in}}\rangle = \sum_i c_i^o |\mathbf{v}_i\rangle$  into the output state  $|\psi_{\text{out}}\rangle = \sum_i c_i(v, \ell) |\mathbf{v}_i\rangle$  ( $i, j = 1, \dots, 4$ ), when the atoms have left the set-up, is given by the unitary matrix

$$U_{ij}(v, \ell) = \begin{pmatrix} 1 & 0 & 0 & 0 \\ 0 & \cos\theta(v, \ell) & -i \sin\theta(v, \ell) & 0 \\ 0 & -i \sin\theta(v, \ell) & \cos\theta(v, \ell) & 0 \\ 0 & 0 & 0 & 1 \end{pmatrix}. \quad (21)$$

In this notation, the two-qubit hyperfine basis of the atoms was chosen as

$$|\mathbf{v}_1\rangle = |0, \bar{0}\rangle, |\mathbf{v}_2\rangle = |0, \bar{1}\rangle, \quad (22a)$$

$$|\mathbf{v}_3\rangle = |1, \bar{0}\rangle, |\mathbf{v}_4\rangle = |1, \bar{1}\rangle. \quad (22b)$$

and  $c_i(v, \ell) = \sum_j U_{ij}(v, \ell) c_j^o$ . For different values of the atomic velocity  $v$  and inter-atomic distance  $\ell$ , a different transformation is therefore realized including, for example, the generation of maximally entangled state (4) if

one starts from the initial product state  $|0, \bar{1}\rangle$ . Moreover, we can analyze the atom-atom coupling angle  $\theta(v, \ell)$  for different combinations of  $v$  and  $\ell$  and for its capability to realize non-trivial two-qubit quantum gates. In fact, the suggested set-up is suitable for realizing the i-swap, controlled-Z, and the controlled- $\overline{\text{NOT}}$  quantum gates for different choices of the velocity and distance, together with some slight modifications in the steps that prepare the atoms before entering the cavity-laser system and that brings them back into its ground-state hyperfine levels (see below). In the following, we consider these gates in more details and display their temporal diagrams and possible values  $(v, \ell)$  for which these gates are realized.

### A. i-Swap Gate

Perhaps the simplest quantum gate for performing non-trivial two-qubit operations is the i-swap which is defined by the matrix [23]

$$U_{ij}^{\text{i-swap}} = \begin{pmatrix} 1 & 0 & 0 & 0 \\ 0 & 0 & i & 0 \\ 0 & i & 0 & 0 \\ 0 & 0 & 0 & 1 \end{pmatrix}, \quad (23)$$

in the atomic basis (22). From the comparison of Eqs. (21) and (23), we see that it is straightforward to realize this gate whenever the effective coupling angle between the atoms fulfills the condition

$$\theta(v, \ell) = 3\pi/2 + 2\pi n. \quad (24)$$

Fig. 4(a) displays the various combination of the atomic velocity  $v$  and the inter-atomic distance  $\ell$  which satisfy this condition for  $n = 0, 1, 2$ . For the i-swap gate, moreover, the sequence of steps that needs to be carried out before and after the atoms have crossed the cavity is the same as shown in Figure 2. No additional manipulations are required in order to implement the i-swap gate.

From the viewpoint of experiment, it is of course important to know how stable a gate operation can be performed for small deviations in the  $(v, \ell)$  parameters. This stability can be seen from the fidelity (distance) between the i-swap gate (23) and the unitary matrix (21) that would be obtained for different values of  $(v, \ell)$ . Fig. 4(b) displays the fidelity defined as

$$\begin{aligned} F_{\text{i-swap}}(v, \ell) &\equiv 1 - \mathcal{N}(\|U(v, \ell) - U^{\text{i-swap}}\|) \\ &= 1 - \sqrt{\frac{1 + \sin \theta(v, \ell)}{2}}, \end{aligned} \quad (25)$$

where  $\|M\| \equiv \sqrt{\text{Tr}(M M^\dagger)}$  is the *Frobenius* norm [24] and  $\mathcal{N}(f_{x,y}) \equiv f_{x,y} \cdot \text{Max}(f_{x,y})^{-1}$  is used for its normalization upon the interval  $0 \leq F_{\text{i-swap}} \leq 1$ .

By construction, this fidelity is a continuous function for which the realization of the i-swap gate occurs when  $F_{\text{i-swap}}(v, \ell) = 1$ , which corresponds to the values  $(v, \ell)$  displayed in Fig. 4(a).

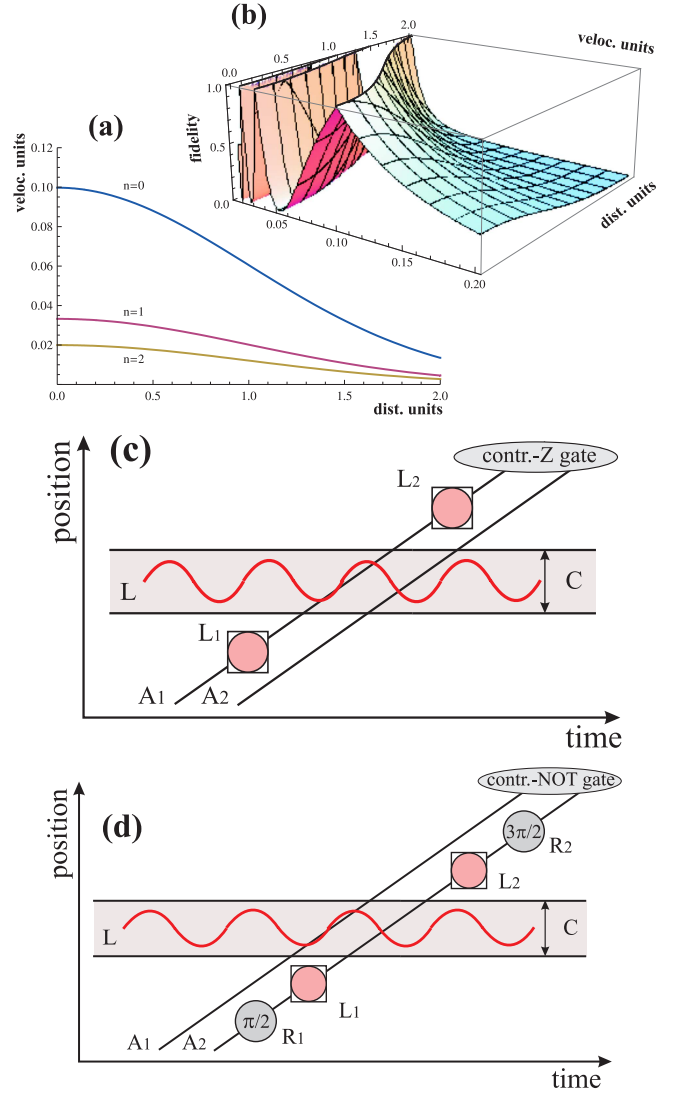


FIG. 5: (Color online) (a) Combinations of the atomic velocity  $v$  and inter-atomic distance  $\ell$  that realizes the controlled-Z (27) and the controlled- $\overline{\text{NOT}}$  (32) gates, i.e., that satisfy the conditions (29) and (36) for  $n = 0, 1, 2$ . (b) Fidelity  $F_{\text{CZ}}(v, \ell)$  as function of the atomic velocity  $v$  and inter-atomic distance  $\ell$ . The same units of  $v$  and  $\ell$  are used as in Fig. 3. (c) Temporal diagram for generating the controlled-Z gate for the two hyperfine qubits of the atoms  $A_1$  and  $A_2$ . (d) The same as in Fig. 5(c) but for the controlled- $\overline{\text{NOT}}$  gate.

### B. Controlled-Z Gate

For two interacting qubits  $A$  and  $B$ , the controlled-Z gate is defined by the transformation [22]

$$U_{\text{CZ}}|\alpha_A, \beta_B\rangle = (-1)^{\alpha\beta}|\alpha_A, \beta_B\rangle, \quad (26)$$

where  $\alpha, \beta = 0, 1$  are the basis states. This gate is a simple example for a conditional quantum dynamics which introduces an additional phase  $e^{i\pi} = -1$  whenever both qubits are in the state  $|1_A, 1_B\rangle$ .

In Sec. II, we concluded that the initial product state  $|1, \bar{1}\rangle$  of the two atoms does *not* undergo any evolution mediated by the cavity-laser fields. Therefore, the direct identification of the atomic hyperfine states  $|0\rangle$ ,  $|1\rangle$  and  $|\bar{0}\rangle$ ,  $|\bar{1}\rangle$  with the (logical) qubit states  $|0_A\rangle$ ,  $|1_A\rangle$  and  $|\bar{0}_B\rangle$ ,  $|\bar{1}_B\rangle$  in (26) will not allow us to realize the control-Z gate, while the reversed assignment for qubit  $A$

$$|0\rangle = |1_A\rangle, \quad |1\rangle = |0_A\rangle, \quad |\bar{0}\rangle = |0_B\rangle, \quad |\bar{1}\rangle = |1_B\rangle.$$

would do so. With this assignment of the basis (22), the transformation matrix for the requested controlled-Z gate is

$$U_{ij}^{CZ} = \begin{pmatrix} 1 & 0 & 0 & 0 \\ 0 & -1 & 0 & 0 \\ 0 & 0 & 1 & 0 \\ 0 & 0 & 0 & 1 \end{pmatrix}. \quad (27)$$

In contrast to the i-swap gate (23), however, the matrix (27) cannot be obtained from the evolutionary matrix (21) by just imposing a condition of the type (24) on the coupling angle  $\theta(v, \ell)$ . Instead, we must consider here the new temporal diagram as displayed in Fig. 5(c). The difference between this diagram and the sequence from Fig. 2 is that the second atom  $A_2$  is not subjected to the Raman pulses  $L_1$  and  $L_2$ , implying that its (hyperfine) state  $|\bar{0}\rangle$  is not mapped upon the (optical) state  $|\bar{a}\rangle$  nor that it need to be brought back. In the suggested set-up in Fig. 1(c), for instance, this modification is realized quite simply by switching off the pairs of Raman laser beams while the atom  $A_2$  crosses the zones  $L_1$  and  $L_2$ .

Following the temporal sequence in Fig. 5(c) and by making use of Eq. (16), we see that the four input states will evolve (for  $t \rightarrow +\infty$ ) into

$$\begin{aligned} |0, \bar{0}\rangle &\rightarrow |0, \bar{0}\rangle, \\ |0, \bar{1}\rangle &\rightarrow \cos\theta(v, \ell)|0, \bar{1}\rangle - i \sin\theta(v, \ell)|1, \bar{a}\rangle, \\ |1, \bar{0}\rangle &\rightarrow |1, \bar{0}\rangle, \\ |1, \bar{1}\rangle &\rightarrow |1, \bar{1}\rangle. \end{aligned} \quad (28)$$

when both atoms passed through the set-up. Although, in general, the output state in the second line does not belong to the basis set (22), the transformation matrix (27) is obtained whenever the condition

$$\theta(v, \ell) = \pi + 2\pi n, \quad (29)$$

is fulfilled. In this case, the unwanted part  $|1, \bar{a}\rangle$  in the second line vanishes. Fig. 5(a) displays the values of  $v$  and  $\ell$  for which the condition (29) is satisfied. Moreover, by applying the fidelity we introduced in Section III. A, the fidelity between the ideal gate (27) and the effective transformation (28) takes the form

$$F_{CZ}(v, \ell) = 1 - \sqrt{\frac{1 + \cos\theta(v, \ell)}{2}}, \quad (30)$$

and is displayed in Fig. 5(b) for different values of  $v$  and  $\ell$ . As for the i-swap gate (23), the least rapid change in the fidelity occurs along the  $n = 0$  lines and, in particular, for small interatomic distances but moderate velocities.

### C. Controlled- $\overline{\text{NOT}}$ Gate

For two interacting qubits  $A$  and  $B$ , the controlled- $\overline{\text{NOT}}$  gate is defined by the transformation [25]

$$U_{CN} = |0_A\rangle\langle 0_A| \times I^B - |1_A\rangle\langle 1_A| \times U_{\text{not}}^B \quad (31)$$

where  $I^B = |0_B\rangle\langle 0_B| + |1_B\rangle\langle 1_B|$  is the identity matrix and  $U_{\text{not}}^B = |0_B\rangle\langle 1_B| + |1_B\rangle\langle 0_B|$  denotes the single-qubit NOT gate associated with the qubit  $B$ . As for the standard controlled-NOT gate, we shall refer to the qubits  $A$  and  $B$  as the *control* and *target* qubit, respectively. While the control qubit does not change its state under the gate (31), the target qubit is swapped together with the phase factor  $e^{i\pi} = -1$  when the control qubit is set to  $|1_A\rangle$ . In the basis (22), the controlled- $\overline{\text{NOT}}$  gate is therefore given by the matrix

$$U_{ij}^{\text{CN}} = \begin{pmatrix} 1 & 0 & 0 & 0 \\ 0 & 1 & 0 & 0 \\ 0 & 0 & 0 & -1 \\ 0 & 0 & -1 & 0 \end{pmatrix}, \quad (32)$$

if the assignment

$$|0\rangle = |0_A\rangle, \quad |1\rangle = |1_A\rangle, \quad |\bar{0}\rangle = |0_B\rangle, \quad |\bar{1}\rangle = |1_B\rangle$$

is utilized.

Obviously, the matrix (32) can not be obtained from the evolutionary matrix (21) by just imposing a single restriction on the coupling angle  $\theta(v, \ell)$ . Hence we consider the modified temporal diagram displayed in Fig. 5(d). According to this diagram, the control atom  $A_1$  is not subjected to the Raman pulses  $L_1$  and  $L_2$ , however, the target atom  $A_2$  passes through two additional classical microwave fields, where each field gives rise to a (coherent) superposition of atomic hyperfine states due to

$$|\bar{0}\rangle \rightarrow \cos(\eta/2)|\bar{0}\rangle - \sin(\eta/2)|\bar{1}\rangle \quad (33a)$$

$$|\bar{1}\rangle \rightarrow \sin(\eta/2)|\bar{0}\rangle + \cos(\eta/2)|\bar{1}\rangle \quad (33b)$$

with a microwave pulse duration  $\tau \sim \eta$ . In the literature, such an atom-field interaction is often called a Ramsey pulse and is denoted in Fig. 5(d) by grey circles. These circles contains the interaction time in units of Ramsey rotations  $\eta$ , and the letters  $R_1$  and  $R_2$  are associated with the Ramsey zones in front and behind of the cavity [see Fig. 1(c)].

Making use of Fig. 5(d) and Eqs. (33), the state of  $A_2$  is first transformed to

$$|\bar{0}\rangle \xrightarrow{\pi/2} \frac{1}{\sqrt{2}}(|\bar{0}\rangle - |\bar{1}\rangle) \quad \text{or} \quad |\bar{1}\rangle \xrightarrow{\pi/2} \frac{1}{\sqrt{2}}(|\bar{0}\rangle + |\bar{1}\rangle) \quad (34)$$

by using a  $\pi/2$  Ramsey pulse in the zone  $R_1$ . Before the atom then enters the cavity, the atomic hyperfine state  $|\bar{0}\rangle$  is mapped upon the optical state  $|\bar{a}\rangle$  by means of the Raman pulse  $L_1$ . Overall, this gives rise to the superposition

$$|\bar{0}\rangle \xrightarrow{\pi/2}_{L_1} \frac{1}{\sqrt{2}}(|\bar{a}\rangle - |\bar{1}\rangle) \quad \text{or} \quad |\bar{1}\rangle \xrightarrow{\pi/2}_{L_1} \frac{1}{\sqrt{2}}(|\bar{a}\rangle + |\bar{1}\rangle).$$

Inside the cavity, as outlined above, only the product state  $|1, \bar{a}\rangle$  of the two atoms evolves according to Eq. (19). This makes the target qubit  $A_2$  to remain unchanged if the control qubit  $A_1$  was set initially to  $|0\rangle$ . If in contrast, the control qubit was set to  $|1\rangle$ , then the effective atom-atom evolution (19) applies and gives rise to a swap of the target qubit  $A_2$  for a proper choice of the velocity  $v$  and the inter-atomic distance  $\ell$ . When both atoms have passed through the cavity, the state  $|\bar{a}\rangle$  is mapped back to  $|\bar{0}\rangle$  by the Raman pulse  $L_2$  and, finally, the atom  $A_2$  is subjected to a  $3\pi/2$  Ramsey pulse in the zone  $R_2$ .

The Ramsey and Raman pulses from above together with the cavity-laser mediated atom-atom interaction make, therefore, the four input states of the hyperfine qubits to evolve ( $t \rightarrow +\infty$  and up to global phase factor)

$$|0, \bar{0}\rangle \rightarrow |0, \bar{0}\rangle, \quad (35a)$$

$$|0, \bar{1}\rangle \rightarrow |0, \bar{1}\rangle, \quad (35b)$$

$$|1, \bar{0}\rangle \rightarrow \frac{(1 + \cos\theta(v, \ell))}{2}|1, \bar{0}\rangle - \frac{(1 - \cos\theta(v, \ell))}{2}|1, \bar{1}\rangle + i \sin\theta(v, \ell) \frac{(|a, \bar{0}\rangle - |a, \bar{1}\rangle)}{2}, \quad (35c)$$

$$|1, \bar{1}\rangle \rightarrow \frac{(1 + \cos\theta(v, \ell))}{2}|1, \bar{1}\rangle - \frac{(1 - \cos\theta(v, \ell))}{2}|1, \bar{0}\rangle + i \sin\theta(v, \ell) \frac{(|a, \bar{0}\rangle - |a, \bar{1}\rangle)}{2}, \quad (35d)$$

once the atoms are sufficiently far away from the set-up.

Although, again, the output states in the last two lines do not belong to the basis set (22), the matrix (32) can be realized if we impose the condition

$$\theta(v, \ell) = \pi + 2\pi n, \quad (36)$$

for the effective coupling angle. Since it is the same condition as Eq. (29) for the controlled-Z gate, the combinations of  $v$  and  $\ell$  that are appropriate for the controlled- $\overline{\text{NOT}}$  gate are displayed already in Fig. 5(a) for  $n = 0, 1, 2$ , and the same applies also for the fidelity between the ideal controlled- $\overline{\text{NOT}}$  gate and the effective transformation (35) in Fig. 5(b).

#### IV. SUMMARY AND OUTLOOK

In summary, a scheme is proposed to generate an entangled state between the hyperfine qubits of two distant non-interacting four-level atoms being separated by the macroscopic distance  $\ell$ . An effective interaction between the atoms is mediated by an off-resonant optical cavity and a laser beam that acts perpendicular to the cavity axis. The purpose of our work is to analyze how the position-dependent coupling of each atom to the same cavity mode and laser affects the interaction among the atoms and whether it is possible to create a (fully) entangled state. In particular, it is shown how the de-

gree of entanglement depends on both, the atomic velocity and the (initial) inter-atomic distance. In addition, schemes are suggested to implement several basic two-qubit quantum gates, such as i-swap gate, controlled-Z, and the controlled- $\overline{\text{NOT}}$  gate in the framework of the given atom-cavity-laser setup. For all these schemes, we display the atomic velocities and inter-atomic distances for which these gates are realized, i.e., the gate fidelities become maximal.

Following the recent experiments [20, 21, 26] and the theoretical works of Refs. [18, 27, 28], the position-dependent effects on the effective atom-atom interaction and entanglement formation mediated by a (detuned) optical cavity, is acknowledged today as a notable step in obtaining the control over the entanglement of atoms within the framework of cavity QED. In particular, Li and coworkers [18] suggested that the distance between atoms is an essential parameter that can be utilized to control the (position-dependent) atom-cavity coupling which implies also the control over the atomic entanglement. However, instead of using a two-level atomic configuration with its strong decoherence effects, it appears more appropriate to consider a four-level  $\Lambda$ -type level configuration in which the quantum information is stored in the hyperfine levels of the atomic ground state. Compared with a recent case study by You *et al.* [13], our scheme differs in that the atoms enter the cavity successively and that a more realistic position-dependent atom-cavity interaction is considered.

One straightforward extension of the effective atom-atom evolution we found in Sec. II, could be the scenario, in which a chain of  $N$  distant four-level atoms cross the experimental setup in Fig. 1(c) and interacts simultaneously with the same cavity mode while passing through the cavity. This extension would lead naturally to the generation of various  $N$ -partite entangled states depending on the  $(v, \ell)$  regime and the succession of Raman and Ramsey zones (see for instance Ref. [29], where we discussed the formation of genuine entangled states for a chain of  $N$  bi-level atoms which cross an analogous experimental set-up we considered in this paper). Finally we remark that an realistic atom-cavity interaction evolution should also include the decoherence effects, which have been avoided in this paper so far. We note that in order to analyze the time evolution of such quantum systems embedded into a reservoir or under the external noise and to analyze different entanglement or separability measures, including those in Eqs. (18) and (25), a quantum simulator has been developed recently in our group [30] that can be utilized for such studies in future.

#### Acknowledgments

This work was supported by the DFG under the project No. FR 1251/13.

- 
- [1] C. H. Bennett and S. J. Wiesner, Phys. Rev. Lett. **69**, 2881 (1992).
- [2] A. K. Ekert, Phys. Rev. Lett. **67**, 661 (1991).
- [3] L. K. Grover, Phys. Rev. Lett. **79**, 325 (1997).
- [4] G. Rempe, Contemp. Phys. **34**, 119 (1993).
- [5] H. J. Kimble, Physica Scripta **T76**, 127 (1998).
- [6] K. J. Vahala, Nature **424**, 838 (2003).
- [7] P. Treutlein, P. Hommelhoff, T. Steinmetz, T. W. Hänsch and J. Reichel, Phys. Rev. Lett. **92**, 203005 (2004).
- [8] C. Langer et al., Phys. Rev. Lett. **95**, 060502 (2005).
- [9] S. Kuhr et al., Phys. Rev. Lett. **91**, 213002 (2003).
- [10] D. Schrader, I. Dotsenko, M. Khudaverdyan, Y. Miroshnychenko, A. Rauschenbeutel and D. Meschede, Phys. Rev. Lett. **93**, 150501 (2004).
- [11] M. P. A. Jones et al., Phys. Rev. A **75**, 040301(R) (2007).
- [12] S. Olmschenk, K. C. Younge, D. L. Moehring, D. N. Matsukevich, P. Maunz and C. Monroe, Phys. Rev. A **76**, 052314 (2007).
- [13] L. You, X. X. Yi and X. H. Su, Phys. Rev. A **67**, 032308 (2003).
- [14] S.-B. Zheng and G.-C. Guo, Phys. Rev. Lett. **85**, 2392 (2000).
- [15] S. Osnaghi et al., Phys. Rev. Lett. **87**, 037902 (2001).
- [16] Y. R. Shen, Phys. Rev. **155**, 921 (1967).
- [17] A. Sørensen and K. Mølmer, Phys. Rev. Lett. **82**, 1971 (1999).
- [18] Y. Li, C. Bruder and C. P. Sun, Phys. Rev. A **75**, 032302 (2007).
- [19] K. M. Fortier, S. Y. Kim, M. J. Gibbons, P. Ahmadi, and M. S. Chapman, Phys. Rev. Lett. **98**, 233601 (2007).
- [20] S. Nussmann, M. Hijlkema, B. Weber, F. Rohde, G. Rempe and A. Kuhn, Phys. Rev. Lett. **95**, 173602 (2005).
- [21] M. Khudaverdyan et al., New J. Phys. **10**, 073023 (2008).
- [22] M. A. Nielsen and I. L. Chuang, *Quantum Computation and quantum Information* (Cambridge University Press, 2000).
- [23] N. Schuch and J. Siewert, Phys. Rev. A **67**, 032301 (2003).
- [24] G. H. Golub and C. F. Van Loan, *Matrix Computations* (Baltimore, Johns Hopkins, 1996).
- [25] In contrast to the controlled- $\overline{\text{NOT}}$  gate we have defined in Eq. (31), the conventional controlled-NOT gate [22]:  $U = |0_A\rangle\langle 0_A| \times I^B + |1_A\rangle\langle 1_A| \times U_{\text{not}}^B$  implies only the flipping of the target qubit (without accumulating a phase) when the control qubit is set to  $|1_A\rangle$ .
- [26] J. K. Pachos and H. Walther, Phys. Rev. Lett. **89**, 187903 (2002).
- [27] J. K. Asbóth, P. Domokos and H. Ritsch, Phys. Rev. A **70**, 013414 (2004).
- [28] S. Natali and Z. Ficek, Phys. Rev. A **75**, 042307 (2007).
- [29] D. Gonta, S. Fritzsche and T. Radtke, Phys. Rev. A **77**, 062312 (2008).
- [30] T. Radtke and S. Fritzsche, Comput. Phys. Commun. **175**, 145 (2006).